

# Imaging With UT1/FORS1: The Fossil Record of Star-Formation in Nearby Dwarf Galaxies

E. TOLSTOY<sup>1</sup>, J. GALLAGHER<sup>2</sup>, L. GREGGIO<sup>3</sup>, M. TOSI<sup>3</sup>, G. DE MARCHI<sup>1</sup>  
M. ROMANIELLO<sup>1</sup>, D. MINNITI<sup>4</sup>, A. ZIJLSTRA<sup>5</sup>

<sup>1</sup>ESO; <sup>2</sup>University of Wisconsin, Madison, WI, USA; <sup>3</sup>Bologna Observatory, Italy;  
<sup>4</sup>Universidad Católica, Santiago, Chile; <sup>5</sup>UMIST, Manchester, United Kingdom

## Abstract

In August 1999 we used FORS1 on UT1 in excellent seeing conditions over three nights to image several nearby galaxies through the B and R broadband filters. The galaxies observed, Cetus, Aquarius (DDO 210) and Phoenix, were selected because they are relatively close-by, open-structured dwarf irregular or spheroidal systems. Owing to the excellent seeing conditions we were able to obtain very deep exposures covering the densest central regions of these galaxies, without our images becoming prohibitively crowded. From these images we have made very accurate Colour-Magnitude Diagrams of the resolved stellar population down below the magnitude of the Horizontal Branch region. In this way we have made the first detection of Red Clump and/or Horizontal Branch populations in these galaxies, which reveal the presence of intermediate and old stellar populations. In the case of Phoenix, we detect a distinct and populous blue Horizontal Branch, which indicates the presence of quite a number of stars >10 Gyr old. These results further strengthen evidence that most, if not all, galaxies, no matter how small or metal poor, contain some old stars. Another striking feature of our results is the marked difference between the Colour-Magnitude diagrams of each galaxy, despite the apparent similarity of their global morphologies, luminosities and metallicities. For the purposes of accurately interpreting our results we have also made observations in the same filters of a Galactic globular cluster, Ruprecht 106, which has a metallicity similar to the dwarf galaxies.

## 1. Introduction

Deep Colour-Magnitude Diagrams (CMDs) of resolved stellar populations provide powerful tools to follow galaxy evolution directly in terms of physical parameters such as age (star formation history, SFH), chemical composition and enrichment history, initial mass function, environment, and dynamical

history of a system. Some of the physical parameters that affect a CMD are strongly correlated, such as metallicity and age, since successive generations of stars may be progressively enriched in the heavier elements. Thus, detailed numerical simulations of CMD morphology are necessary to disentangle the complex effects of different stellar populations overlying each other and make an effective quantitative analysis of possible SFHs (e.g., Tosi et al. 1991; Tolstoy and Saha 1996; Dohm-Palmer et al. 1997). For every galaxy for which an accurate CMD has been derived, down to the Horizontal Branch (HB) luminosity ( $M_R \sim 0. \pm 0.5$ ) or fainter we have learnt something new and fundamentally important about the SFH that was not discernable from images containing the red giant branch (RGB) alone (e.g., Smecker-Hane et al. 1994; Tolstoy et al. 1998; Cole et al. 1999).

Accurate CMD analysis benefits enormously from the high spatial resolution and excellent image quality, as crowded-field stellar photometry is ex-

tremely sensitive to seeing, which affects both the degree of crowding and the speed with which an image becomes sky noise limited. Previous programmes on ESO telescopes have been carried out with the 2.2-m telescope (e.g., Tosi et al. 1989) and more recently with the NTT (e.g., Minniti and Zijlstra 1996). Here we show that in ideal conditions, and with a large, high-performance telescope and closed-loop active optics spectacular improvements can be obtained on previous results.

Because of the significant gains in image quality and collecting area now available with the VLT on Paranal, it is worthwhile and fundamentally important to survey resolved stellar populations down to the HB of all nearby galaxies in our Local Group and beyond (see Fig. 1). This will provide a uniform picture of the evolutionary properties of galaxies with a wide variety of mass, metallicity, gas content, etc. and thus guide our understanding of galaxy evolution in conditions of extremely low metallicity, presumably similar to those

**Table 1: The Sample**

Object	Distance (kpc)	$M_V$	[Fe/H] (dex)	type	ref
Aquarius	800	-10.0	-1.9	dl/dSph	Mateo 1998
Phoenix	445	-10.1	-1.9	dl/dSph	Mateo 1998
Cetus	800	-10.1	-1.7	dSph	Whiting et al. 1999
Ruprecht 106	20	-6.45	-1.7	globular cluster	Da Costa et al. 1992

**Table 2: The Observations**

Galaxy	date	filter	exp. time (secs)	<seeing> (arcsec)
Aquarius	17Aug99	R	3000	0.45
		B	3600	0.45
Phoenix	19Aug99	R	1600	0.80
		B	1800	0.80
Cetus	17Aug99	R	3000	0.45
		B	3600	0.55
Ruprecht 106	19Aug99	R	30	0.60
		B	80	0.75

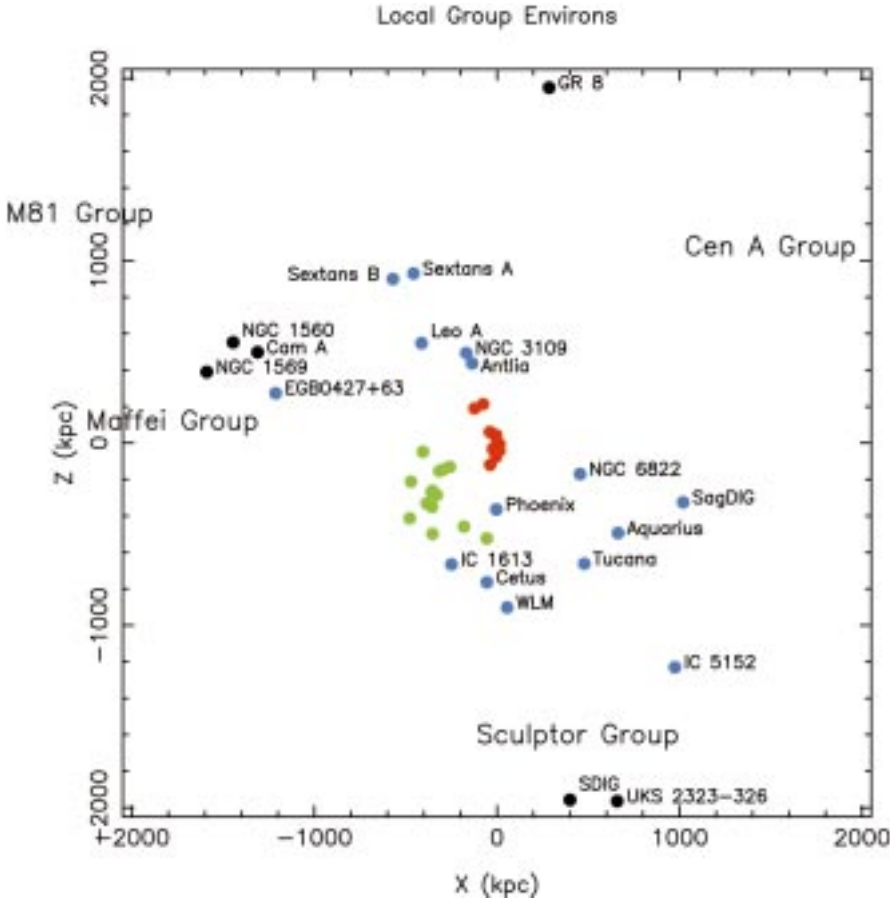


Figure 1: The spatial distribution of the Local Group plus neighbouring galaxies in X-Z galactic coordinates. Our Galaxy is at the origin of this plot, and our dwarf spheroidal neighbours are all marked by red dots. M31 and its colony of neighbouring dwarf ellipticals and spheroidals are marked in green. The more free-floating dwarf irregular/spheroidal galaxy components of the Local Group are marked in light blue dots (including Aquarius, Phoenix and Cetus) and also labelled. In black are the more distant galaxies on the fringes of the Local Group. This figure was kindly provided by Mike Irwin, and comes from Whiting et al. (1999).

expected in the early Universe. A complete survey of the SFH of the nearby Universe should also be broadly consistent with those determined from high redshift surveys (e.g., Steidel et al. 1999).

## 2. The Sample

Despite the advances in ground-based image quality at the VLT, we still have to carefully select galaxies that will be relatively uncrowded, i.e. systems with a stellar density of 0.01–0.5 stars/arcsec<sup>2</sup>, down to the magnitude of the HB region. Dwarf Irregular (dI) and Spheroidal (dSph) galaxies at 400–800 kpc distance fit perfectly into this category (see Table 1). These types of galaxies are also the most numerous in the Local Group (see Fig. 1) and beyond, and there is considerable evidence for widely varying evolutionary histories, with periods of active star formation interspersed with quiescent periods (e.g., Smecker-Hane et al. 1994; Gallart et al. 1999). They have thus been suggested as good candidates for present-day counter-parts to the “faint blue galaxies” seen in redshift surveys

(e.g., Ellis 1997). Two of the objects we looked at are known as “transition” objects, which means they are intermediate in class between dSph (no current star formation, or HI gas) and dIs (current star formation and HI gas), and are particularly interesting because they may help us to understand why galaxies may turn on and off their star-formation process galaxy-wide and thus why dwarf galaxies can exhibit such widely differing SFHs.

## 3. The Observations

Our observing run, from 17–19 August 1999, had varying seeing conditions (0.3”–0.9” on the seeing monitor), but there were several periods lasting 1–2 hours with stable, excellent seeing. It was these periods which we used to image the resolved stellar populations of nearby galaxies. At other times we observed in narrow-band filters, or went to a separate programme of spectroscopy of individual stars in nearby galaxies. We present the data for three of the galaxies we imaged during our run (see Table 2). The sensitivity characteristics of the FORS1 CCD

(Tektronix) led us to observe in B and R filters. The B filter is very useful for characterising HB morphology, especially the blue HB.

We typically split our observations into short (500–600 sec) dithered groups of images to help minimise flat-fielding problems and removal of cosmic rays and bad pixels. The readout characteristics of the CCD with FIERA (4-port readout in 27 secs, with a read noise of  $\sim 6 e^-$ ) make this an efficient way to observe. To make an accurate photometric solution, we made observations at a different airmass of a standard field (PG1657) containing several stars over a large range in colour ( $B - R = -0.21$ – $1.64$ ) on our first night. We then observed two fields (PG1657 and PG2331) on the second night and one on the third at airmass close to those at which our observations were made to confirm that the photometric solution obtained on night 1 was stable all through our run, and to confirm that all three nights were clear and photometric. The photometric solution is:

$$R - R' = 27.38 - 0.018 * X - 0.025 * (B' - R')$$

$$B - B' = 27.21 - 0.213 * X - 0.039 * (B' - R')$$

where  $R'$  and  $B'$  are the observed magnitudes (in  $e^-/s$ ),  $R$  and  $B$  are the true magnitudes, and  $X$  is the airmass. In Figure 2 we show the central 4 arcmin of the combined 3600 sec of B filter imaging of Cetus. The average FWHM of the more than 11,000 stars “photometered” over the whole 6.8 arcmin FORS1 image is 0.45”. All the extended objects visible in Figure 2 are distant galaxies *behind* Cetus.

## 4. Results

We carried out PSF fitting photometry using a modified version of DoPHOT, following the precepts laid out by Saha et al. (1996), over each of our reduced and combined images, and matched the stars detected with sufficient signal-to-noise in both filters. The resulting calibrated but not reddening corrected CMDs are shown in Figure 3. These are the most detailed CMDs ever made from the ground of such distant systems.

In each CMD in Figure 3 we have clearly detected the Red Clump (RC) / HB region ( $M_R \sim 0 \pm 0.5$ ). This region contains an evolutionary sequence of Helium Burning low-mass stars 1 Gyr and older. The relative number of stars in each phase determines the age mix of the stellar populations older than 1 Gyr. There is a clear diversity of morphologies in Figure 3, where each galaxy (and the globular cluster) are all distinctly different suggesting quite different past SFHs.

The *Aquarius dwarf* which was also studied in the original ESO-MPI/2.2-m study (Greggio et al. 1993), has recently been shown to be at a distance consistent with Local Group membership (Lee et al. 1999). Its CMD (Fig. 3a) has a narrow RGB ( $B - R > 1.2$ ), and what looks like a relatively young RC ( $M_R \sim -0.5$ ,  $B - R \sim 1.1$ ), and very little, if any, older HB population. It also has evidence of a fairly young stellar population from He burning blue loop stars (sequence going left to right in the CMD between  $M_R \sim -4$  and  $-0.5$  and in colour  $B - R \sim 0$  and  $1$  and intersecting with the RC) and a main sequence (vertically at  $M_R \sim 0$ ). Aquarius thus appears to resemble Leo A, a galaxy which is completely dominated by stars younger than 2 Gyr (Tolstoy et al. 1998).

The *Phoenix dwarf* CMD (Figure 3b) has an extraordinarily complex HB and possibly an overlying, young RC. The distinct and well populated blue HB (at  $M_R \sim 0$  and  $B - R \sim 0 \pm 0.2$  to  $B - R \sim 0.4$ ) is an unambiguous indication that this galaxy contains quite a number of stars that are older than 10 Gyr. There are also a sprinkling of young main-sequence and blue loop stars, as defined for Aquarius. This looks like a galaxy that has been forming stars, perhaps on and off, for a Hubble time.

The *Cetus dwarf* is a newly discovered member of the Local Group (Whiting et al. 1999). From this CMD (Fig. 3c) it looks like it may contain a blue HB population, although much less prominent than the one in Phoenix. It has a very densely populated red HB/RC (lying between  $B - R \sim 0.5$  and  $1.2$ ), with a lot of structure that might resemble that predicted in the recent models of Girardi (1999). This galaxy is probably predominantly of intermediate age, and there is no evidence for star formation in the last 1.5 Gyr or so.

*Ruprecht 106*, a Galactic globular cluster, known to have a similar metallicity as these galaxies (Da Costa et al. 1992), was also observed as a basic test of our calibration and modelling procedures. From the CMD (Fig. 3d) we made an RGB and an HB fiducial line, to facilitate the comparison between it and the galaxy CMDs. These lines are overplotted in red on each of the galaxy CMDs in Figure 3. The normalisation is somewhat arbitrary because careful modelling has not yet been made to ascertain the optimum reddening and distances with these new accurate CMDs. *Ruprecht 106* is a single old population (12–13 Gyr old), whereas all the galaxies are composite with a spread of age and/or metallicity broadening their HB/RC and RGB. However, *Ruprecht 106* serves as a good starting point to characterise the properties of each galaxy, and we will also use it to help determine how accurate the theoretical isochrones are.



Figure 2: This is a 4' square piece of a FORS1 image in the centre of the *Cetus dwarf* galaxy, taken through the B filter. It is the composite of six 600sec images. Each image was registered to the nearest pixel and co-added. On the resulting images the stellar sources have a PSF measuring FWHM  $\sim 0.45''$ . The extended sources seen in this image are galaxies behind *Cetus*.

## 5. Interpreting Colour-Magnitude Diagram Morphology

These data will be fully interpreted using quantitative synthetic modelling techniques – making use of theoretical stellar evolution tracks (e.g., Girardi et al. 2000) and, where possible, globular/open cluster observations.

The Main-Sequence and Blue-Loop stars are fairly straightforward indicators of what the star formation rates have been in these galaxies for the last 0.5–1 Gyr. The RGB is an indicator of star formation which has taken place more than  $\sim 1$  Gyr ago. Unfortunately it is not straight forward to disentangle the details of the precise SFH more than 1 Gyr ago because of difficulties like the age-metallicity degeneracy. That the galaxy RGBs are spread in colour in comparison to *Ruprecht 106* RGB is clear, but the effects which cause this can be either or both of age and metallicity variations.

We can obtain additional information on the older populations from the RC/HB populations. The RC evolves strongly with age through the 1–6 Gyr age range (Caputo et al. 1995, Tolstoy 1998), and if we are lucky enough to have a population in this age range, quite a lot can be said about the SFH of

this galaxy. After about 6–8 Gyr, we start to see a red HB extension to the RC. This feature in *Cetus* and *Phoenix* probably means that in addition to RC populations a few Gyr old, there are also populations older than  $\sim 6$  Gyr. In the case of *Phoenix* the presence of a blue HB population is a definitive indicator of an ancient stellar population older than 10 Gyr.

However, although the HB region of a CMD provides the brightest unambiguous indicators of old and intermediate stellar populations, it is difficult to use them to uniquely quantify ancient star formation rates. Basically the problem is that the colour spread of observed HBs cannot be reproduced by theoretical isochrones without invoking variable amounts of mass loss from the RGB progenitors. This is often called the “Second Parameter Effect” (e.g., Fusi Pecci & Bellazzini 1997) which results in some metal poor clusters having redder HBs than models of their metallicity would predict. Thus it is possible for globular clusters of identical age and metallicity to have very different HBs. The implications for a composite population in a galaxy of unknown age and metallicity variations are clearly dire. However, careful modelling of the number of stars on a HB

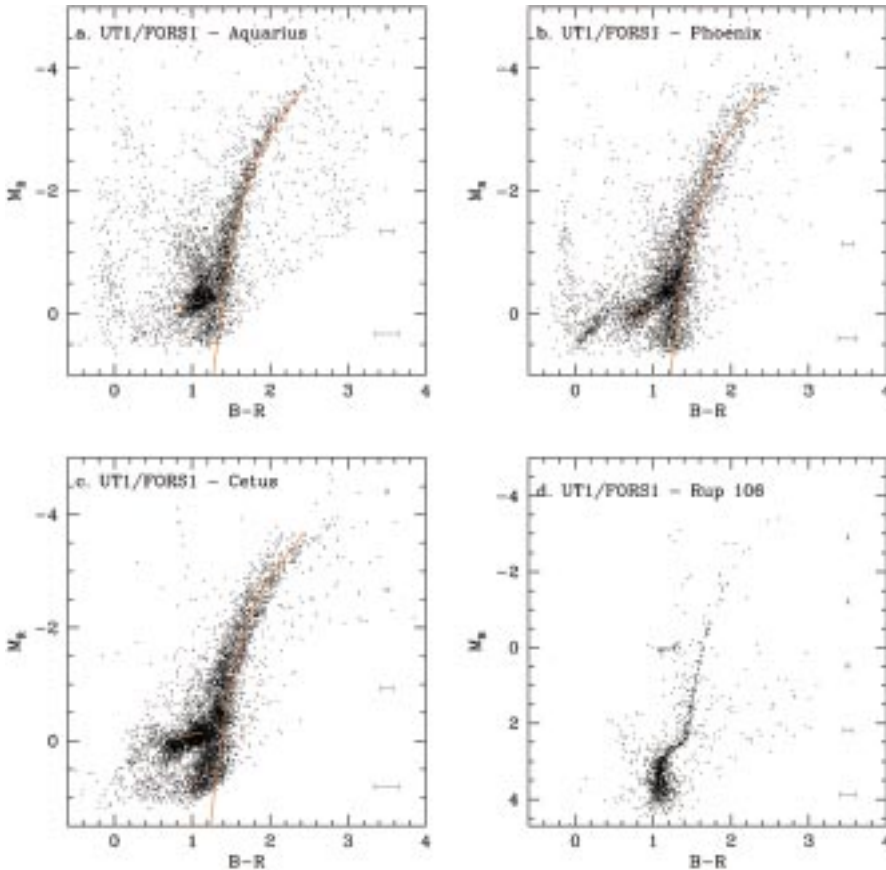


Figure 3: Here are plotted the Colour-Magnitude Diagrams which resulted from the data summarised in Table 2 for the Cetus, Aquarius and Phoenix dwarf galaxies, and the globular cluster Ruprecht 106. Representative error bars are also plotted for each data set. These data have not been corrected for any reddening effects. From the Ruprecht 106 data a fiducial mean was found for the ROB and HB. This is then overplotted on each of the galactic CMDs in red. An accurate fit has not been made, these have just been overlaid on each CMD for the purposes of comparison only. Before accurate conclusions can be drawn a detailed analysis of the reddening and distance uncertainties in all cases have to be made.

(and not where they lie) in conjunction with the RC and the RGB can constrain the plausible SFHs and put limits on the number of stars which could have been formed more than 6–8 Gyr ago, even if the precise SFH at these times cannot be extracted (e.g., Han et al. 1997; Gallagher et al. 1998; Tolstoy et al. 1998; Tolstoy 1998). The ratio of red to blue HB stars can also be used as an indicator of the age and metallicity spread of the oldest stellar populations in a galaxy (e.g., Da Costa et al. 2000).

## 6. Summary

The earliest epochs of star formation in the Universe must have occurred in low-metallicity environments. The only place where we can study on-going extremely low metallicity star formation in detail is in nearby dwarf irregular galaxies. They typically have metallicities in the range 3–10% of solar values (e.g., Skillman et al. 1989). Looking at galaxies which appear to be in transition between a period of star formation and a period of quiescence may help to determine what can effect star formation on a galaxy wide-scale (albeit a small galaxy) and result in the tre-

mendous diversity of SFHs seen in dwarf galaxies.

The SFH of the nearby universe should also reflect that determined from redshift surveys (e.g., Steidel et al. 1999). To make this comparison an accurate one, we need data like these to determine when nearby galaxies, even the smallest ones, formed most of their stars and if bursts were ever common enough or bright enough to produce faint blue galaxies at intermediate redshifts (e.g., Tolstoy 1998). The giant galaxies (M 31, the Galaxy, M 33) contain something like 90% of the stellar mass in the Local Group, so this is undeniably where the dominant mode of star formation occurs. However, the concern remains that, because the properties of faint blue galaxies resemble more late-type irregular galaxies, the redshift surveys are picking up dwarf systems which are very bright for only a short time and do not constitute a significant fraction of the star formation in the universe (e.g., Fukugita et al. 1998, Tolstoy 1998).

To date, the limiting factors in determining accurate SFHs in the Local Group have been crowding, sensitivity and resolution limits for accurate stellar

photometry. HST first showed us the magnificent improvements in understanding SFHs from CMDs made possible by high-resolution imaging (e.g., Tolstoy 1999). The large collecting area and impressive image quality and stability of UT1 combined with the extremely good seeing attainable at Paranal makes it possible to obtain accurate CMDs of relatively uncrowded dl/dSph systems. FORS1 also allows us to extend our knowledge of faint stellar populations into the blue, something with which HST has difficulty, and also to image the entire area of a dwarf galaxy (typically 3–5' across) in one shot. FORS1 is thus an extremely important complement to WFPC2 on HST, which is needed to push deeper down the main sequence to detect faint main-sequence turnoffs to quantify the contribution of the older populations seen in the HB. FORS imaging would inevitably have crowding problems at these faint magnitudes and with the increase in crowding.

We have shown that under good conditions the VLT can deliver high-quality images that result in exquisitely detailed CMDs which can be used to determine the SFHs of all the galaxies in our Local Group and ways beyond. It is also worth looking further afield to start surveying the high-mass stellar populations of other groups.

**Acknowledgements:** We thank the support staff at Paranal Observatory (particularly Thomas Szeifert, Andreas Kaufer and Chris Lidman) who helped us to make very efficient use of the telescope.

## References

- Caputo F., Castellani V. & Degl'Innocenti S. (1995) *A&A*, **304**, 365.
- Cole A.A., Tolstoy E., Gallagher J.S., Hoessel J.G., Mould J.R., Holtzman J.A., Saha A., & the WFPC2 IDT team 1999 *AJ*, **118**, 1657.
- Da Costa G.S., Armandroff T.E. & Norris J.E. 1992 *AJ*, **104**, 154.
- Da Costa G.S., Armandroff T.E., Caldwell N. & Seitzer P. 2000 *AJ*, in press (astro-ph/9911020).
- Dohm-Palmer R.C., Skillman E.D., Saha A., Tolstoy E., Mateo M., Gallagher J.S., Hoessel J. & Chiosi C. 1997 *AJ*, **114**, 2514.
- Ellis R. 1997 *ARAA*, **35**, 389.
- Fukugita M., Hogan C.J. & Peebles P.J.E. (1998) *ApJ*, **503**, 518.
- Fusi-Pecci F. & Bellazzini M. 1997 *Third Conference on Faint Blue Stars*, in press (astro-ph/9701026).
- Gallagher J.S., Tolstoy E., Saha A., Hoessel J., Dohm-Palmer R.C., Skillman E.D. & Mateo M. 1998, *AJ*, **115**, 1869.
- Gallart C., Freedman W.L., Aparicio A., Bertelli G. & Chiosi C. 1999 *AJ*, **118**, 2245.
- Girardi L. 1999 *MNRAS*, **308**, 818.
- Girardi L., Bressan A., Bertelli G. & Chiosi C. 2000 *A&A*, **141**, 371.
- Greggio L., Marconi G., Tosi M. & Focardi P. 1993 *AJ*, **105**, 894.
- Han M., Hoessel J.G., Gallagher J.S., Holtzman J. & Stetson P.B. 1997, *AJ*, **113**, 1001.

Minniti D. & Zijlstra A. 1996 *ApJ*, **467**, L13.  
 Lee M.G., Aparicio A., Tikonov N., Byun Y.-I. & Kim E. 1999 *AJ*, **118**, 853.  
 Saha A., Sandage A., Labhardt L., Tammann G.A., Macchetto F.D. & Panagia N. 1996 *ApJ*, **466**, 65.  
 Skillman E.D., Kennicutt R.C. & Hodge P. 1989 *ApJ*, **347**, 875.  
 Smecker-Hane T.A., Stetson P.B., Hesser J.E. & Lehnert M.D. 1994 *AJ*, **108**, 507.

Steidel C.C., Adelberger K.L., Giavalisco M., Dickinson M. & Pettini M. 1999, *ApJ*, **519**, 1.  
 Tolstoy E. & Saha A. 1996, *ApJ*, **462**, 672.  
 Tolstoy E., Gallagher J.S., Cole A.A., Hoessel J., Saha A., Dohm-Palmer R.C., Skillman E.D., Mateo M. & Hurley-Keller D. 1998, *AJ*, **116**, 1244.  
 Tolstoy E. 1998, XVIIIth Moriond Astrophysics Meeting: *Dwarf Galaxies and*

*Cosmology*, eds. T.X. Thuan et al., in press (astro-ph/9807154).  
 Tolstoy E. 1999, IAU Symposium 192, *The Stellar Content of Local Group Galaxies*, eds. Whitelock & Cannon, p. 218.  
 Tosi M., Focardi P., Greggio L. & Marconi G. 1989, *The Messenger*, **57**, 57.  
 Tosi M., Greggio L., Marconi G. & Focardi P. 1991, *AJ*, **102**, 951.  
 Whiting A.B., Hau G.K.T. & Irwin M. 1999, *AJ*, **118**, 2767.

## FIRES at the VLT: the Faint InfraRed Extragalactic Survey

M. FRANX<sup>1</sup>, A. MOORWOOD<sup>2</sup>, H.-W. RIX<sup>3</sup>, K. KUIJKEN<sup>4</sup>, H. RÖTTGERING<sup>1</sup>,  
P. VAN DER WERF<sup>1</sup>, P. VAN DOKKUM<sup>1</sup>, I. LABBE<sup>1</sup>, G. RUDNICK<sup>3</sup>

<sup>1</sup>Leiden Observatory, <sup>2</sup>ESO, <sup>3</sup>MPIA, <sup>4</sup>University of Groningen

One of the unique capabilities of the VLT is the near-infrared imaging mode of ISAAC. The wide field of view, detector stability, and image quality that ISAAC can provide are currently unparalleled at other observatories.

In order to take advantage of this window of opportunity, we have proposed a non-proprietary, deep imaging survey. The survey consists of very deep exposures in the  $J_s$ , H and  $K_s$  bands of the Hubble Deep Field South (Williams et al. 2000), and somewhat shallower imaging on a wider field in the cluster MS1054-03 at  $z = 0.83$  (Gioia and Luppino 1994, van Dokkum et al. 1999, 2000). The survey is aimed at the study of distant galaxies in both fields, although many other applications will be possible. The same fields are observed at other wavelengths by several other groups. The full complement of data will range from the radio to the X-ray. The fields were selected based on their superb optical imaging from the Hubble Space Telescope. Both fields will be observed for a total of 96 hours, split evenly between  $J_s$ , H and  $K_s$ . In the field of MS1054-03, this integration time will be divided between four pointings to cover the full Hubble Space Telescope mosaic of images (van Dokkum et al. 2000). For the Hubble Deep Field South, one single pointing will cover the WFPC image. The expected depth of the images is a  $K_s$  magnitude of 24.4 (26.3) in the HDF South, and a  $K_s$  magnitude of 23.7 (25.6) in MS1054-03; these are  $3\sigma$  limits in Johnson and AB magnitudes, respectively. The OPC has been very generous and has allocated the full requested time to this survey.

The first data on the Hubble Deep Field South were obtained at the end of 1999. Even the first quarter of the total integration provided  $K_s$ -band data of unprecedented image depth and quality for the HDFs. A colour image is

shown in Figure 1, which is a combination of the HST I band data, and  $J_s$  and  $K_s$  ISAAC data. The variations among the infrared colours of galaxies are striking, and several very red galaxies are immediately apparent in the image.

Some of these galaxies are absent, or very faint in the extremely deep I band data from the Hubble Space Telescope.

Some examples of distant galaxies are shown in Figure 2. The morphologies of the very red galaxies span a

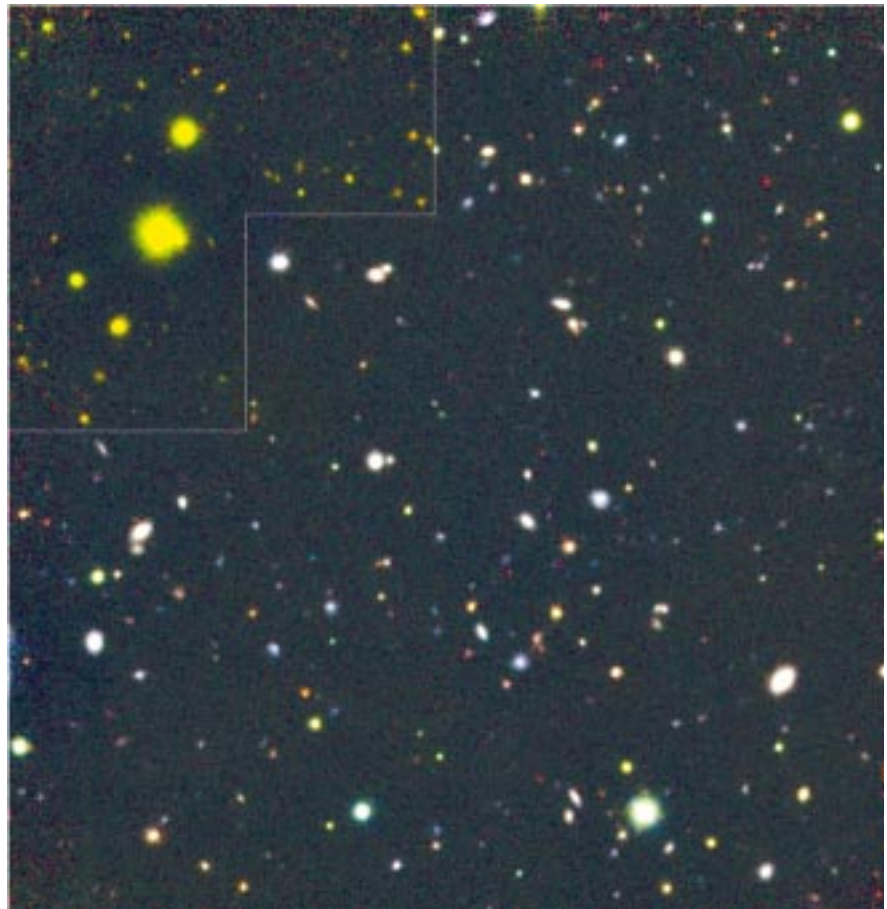


Figure 1. A colour image of the Hubble Deep Field South, observed with the Hubble Space Telescope, and ISAAC on the VLT. The colour image is constructed from the I band images from HST, and the  $J_s$  and  $K_s$  images taken with ISAAC. The outline indicates the size and shape of the WFPC2 field, and the galaxy colours outside of that are yellow-green because of the absence of I band data in the image. The great variety of galaxy colours is striking. These differences are often caused by redshift: at higher redshifts, the Balmer break and 4000 Angstrom break will move in or beyond the bandpass of the I band filter. Some very red galaxies can be identified, these have very low I and  $J_s$  fluxes.